

## 동공부피 분포의 계산결과에 미치는 표면장력의 곡률 의존도 효과

조 창 현·안 운 선\*·장 세 현  
서울대학교 물리과대학 화학과  
(1972. 10. 6 접수)

### Effect of Curvature Dependency of Surface Tension on the Result of Pore-Volume Distribution Analysis

Chang-Hyun Jho, Woon-Sun Ahn\* and Seihun Chang

*Department of Chemistry, Seoul National University*

(Received Oct. 6, 1972)

요 약 질소의 흡착 등온곡선을 이용하여 흡착체의 동공부피 분포를 계산하는 과정에서 표면장력의 곡률 의존도 고려 효과를 조사하였다. 즉, 장세현 등에 의한 표면장력의 곡률 의존도 식과 켈빈 식으로부터 주어진 압력에서의 켈빈반경을 구하고, 이것으로부터 흡착체의 동공부피 분포를 계산하였다. 이와 같이하여 얻은 계산 결과를 표면장력의 곡률 의존도를 고려하지 아니한 종래방법에 의한 계산 결과와 비교하였다.

일반적으로 곡률 의존도를 고려해두면 동공부피 분포 곡선의 극대부분이 큰 동공 쪽으로 이동한다. 또한 모세관 응축이 일어나는 상대압력이 종래까지 생각했던 것보다 훨씬 낮아지고 있다. 이러한 효과들은 흡착체의 동공들이 미세해 질수록 더욱 현저하게 일어난다.

**Abstract** The significance of the curvature dependency correction of surface tension is studied in calculating the pore volume distribution of porous adsorbent from nitrogen adsorption isotherm. That is, Kelvin radii are calculated with curvature dependent surface tension values calculated by Chang et al, and then with these Kelvin radii, pore volume distributions of three porous adsorbents, silica alumina (steam deactivated), silica gel (Davidson 59), and silica gel (Mallinckrodt Standard Luminescent), are calculated. The results are compared with those obtained by the previous method in which surface tension is taken as constant and also with the others obtained by the modelless method proposed by Brunauer et al. The maximum point of the distribution curve shift to the larger pore radius, when the curvature dependency is considered. Furthermore, the relative pressure at which capillary condensation commences is by far the lower than that accepted previously. This effect becomes significant as the pore radius approaches to the micropore range.

#### Introduction

The method of pore volume distribution cal-

culuation of porous substances from the nitrogen adsorption isotherm is developed by Barrett, Joyner, and Halenda<sup>1</sup>. And various refinements have been made by many authors<sup>2,3,4</sup>. Accord-

\*Department of Chemistry, Sung Kyun Kwan University

ing to this method, i) average radius of pores in which capillary condensation takes place at a given finite pressure range is calculated by the use of Kelvin equation, and ii) the amount of capillary condensate in the pore of given radius, hence the pore volume, is calculated from the nitrogen adsorption isotherm.

The amount of nitrogen adsorbed at a given pressure consists of two contributions, one due to the capillary condensation and the other due to the increased multilayer physisorption on the walls of comparatively large vacant pores. Cranston and Inkley<sup>2</sup> have investigated the statistical thickness ( $t$ ) of physisorbed layer on a number of non-porous adsorbents and found that it was converging to a constant value at a given pressure. Assuming an independency of the statistical thickness on the curvature of the walls of adsorbents, they have calculated the contribution of condensate to the total amount of adsorbate at a given pressure, and obtained pore volume distribution curves for a number of adsorbents.

Broekhoff and deBoer<sup>4</sup>, upon the consideration of thermodynamic stability of the physisorbed layer, have shown that the statistical thickness should depend on the curvature of the walls on which physisorption takes place. However, they have shown that the formal thickness of the adsorbed layer on the walls of relatively narrow cylindrical pore is approximately equal to the statistical thickness of the adsorbed layer on the flat surface. In such pores, capillary condensation is expected to take place, before the formal thickness deviates appreciably from the statistical thickness.

On the other hand, the curvature effect on the surface tension is very significant as the curvature increases to the order of  $10^6 \text{ cm}^{-1}$ . Therefore, the vapor pressure in equilibrium with the curved surface, which is obtained from

the Kelvin equation, is quite different depending whether the curvature effect of surface tension is considered or not. For an example, when the pore diameter is about 30 Å, the equilibrium relative vapor pressure is less than 0.130 as can be seen in Table 1, whereas it is 0.350 if the surface tension is assumed to be independent of the curvature.

In this work, pore volume distribution is calculated using the Kelvin equation with curvature dependent surface tension, and the result is compared with the one obtained with the Kelvin equation in which constant surface tension is assumed.

### Curvature Dependency Correction

The radius of closed-end cylindrical pore is calculated by the use of Kelvin equation,

$$r = t - \frac{2\gamma V_m}{RT \ln(P/P_0)} \quad (1)$$

Here,  $P_0$  and  $P$  are the saturation vapor pressure and the vapor pressure at which the capillary condensation takes place in a pore of radius  $r$ , respectively;  $V_m$ , the molar volume of the liquid; and  $\gamma$ , the surface tension of the curved liquid surface. In the application of this equation, the curvature dependency of the surface tension should be known. The effect on the liquid density may be neglected.

Tolman<sup>5</sup>, and Buff and Kirkwood<sup>6</sup> have derived a curvature dependent surface tension equation. Chang et al<sup>7</sup> have also obtained a similar result according to the theory of significant liquid structure;

$$\gamma = \frac{\gamma_\infty}{1 - \frac{2\delta}{r-t}} \quad (2)$$

where,  $\gamma_\infty$  is the surface tension of the flat surface;  $\delta$  is the distance between the surface of separation and the surface of tension accord-

ing to Tolman, and the unimolecular thickness according to Chang et al. The unimolecular thickness can be calculated from the geometrical consideration of molecular packing and solid density. Combining equations (1) and (2), the following equation is obtained.

$$r = t - 2\delta - \frac{2\gamma_{\infty} V_m}{RT \ln(P/P_0)} \quad (3)$$

Using this equation, the radius ( $r$ ) of the closed-end cylindrical pore in which capillary condensation takes place at the relative vapor pressure ( $P/P_0$ ) can be calculated. This radius is converted into the pore diameter and the result is tabulated in the first column of Table 1.

According to Cranston and Inkley, the closed-end cylindrical pore volume ( $V_{12}$ ) whose pore diameters are in the range of  $d_1$  through  $d_2$  is calculated from the following equation;

$$V_{12} = R_{12} \left( v_{12} - k_{12} \sum_{d_2 + \frac{1}{2} \Delta d}^{d_{max}} \frac{d - 2t_{12}}{d^2} V_d \Delta d \right) \quad (4)$$

where,

$$R_{12} = \frac{r_2 - r_1}{\int_{r_1}^{r_2} \frac{(r - t_r)^2}{r^2} dr}$$

$$k_{12} = 4(t_2 - t_1)$$

$$t_{12} = \frac{1}{2}(t_1 + t_2)$$

Table 1. Vanlues of  $P/P_0$ ,  $R_{12}$  and  $k_{12}$  for standard increments of pore diameter.

$d$	$P/P_0$	$k_{12}$	$R_{12}$	$d$	$P/P_0$	$k_{12}$	$R_{12}$
313.4	0.931		1.203	123.4	0.809	1.30	1.449
303.4	0.929	0.50	1.209	113.4	0.787	1.44	1.482
293.4	0.926	0.52	1.215	103.4	0.764	1.60	1.520
283.4	0.924	0.54	1.221	93.4	0.734	1.80	1.565
273.4	0.921	0.56	1.228	83.4	0.696	2.08	1.619
263.4	0.918	0.58	1.235	73.4	0.646	2.44	1.682
253.4	0.915	0.60	1.243	63.4	0.578	1.40	1.736
243.4	0.911	0.62	1.251	58.4	0.535	1.56	1.775
233.4	0.907	0.65	1.261	53.4	0.484	1.76	1.814
223.4	0.902	0.68	1.270	48.4	0.423	2.00	1.852
213.4	0.897	0.71	1.281	43.4	0.350	2.34	1.882
203.4	0.891	0.75	1.293	38.4	0.265	2.86	1.890
193.4	0.885	0.79	1.306	33.4	0.168	1.34	1.873
183.4	0.879	0.84	1.320	31.4	0.130	1.49	1.847
173.4	0.871	0.89	1.336	29.4	0.090	1.68	1.799
163.4	0.861	0.95	1.353	27.4	0.058	1.93	1.729
153.4	0.850	1.02	1.373	25.4	0.035	2.26	1.628
143.4	0.838	1.10	1.395	23.4	0.016		
133.4	0.824	1.19	1.420				

Table 2. The function  $(d-2t)/d^2$  for mean values of  $t$  and  $d$  in each standard increment of pore diameter. (multiply the value by  $10^{-2}$ )

$d$	313.4—153.4	153.4—83.4	83.4—53.2	53.4—48.4	48.4—43.4	43.4—38.4
313.4—303.4	0.301	0.306	0.310	0.311	0.311	0.313
303.4—293.4	0.310	0.315	0.319	0.320	0.321	0.323
293.4—283.4	0.320	0.325	0.330	0.331	0.332	0.334
283.4—273.4	0.331	0.336	0.341	0.342	0.344	0.345
273.4—263.4	0.342	0.348	0.353	0.354	0.356	0.357
263.4—253.4	0.354	0.360	0.366	0.367	0.369	0.370
253.4—243.4	0.367	0.374	0.380	0.381	0.383	0.385
243.4—233.4	0.380	0.388	0.395	0.396	0.398	0.400
233.4—223.4	0.395	0.404	0.411	0.413	0.415	0.417
223.4—213.4	0.411	0.421	0.429	0.430	0.432	0.435
213.4—203.4	0.429	0.439	0.448	0.450	0.452	0.454
203.4—193.4	0.448	0.459	0.469	0.471	0.473	0.476
193.4—183.4	0.468	0.481	0.492	0.494	0.497	0.500
183.4—173.4	0.491	0.505	0.517	0.519	0.522	0.526
173.4—163.4	0.515	0.531	0.545	0.548	0.551	0.555
163.4—153.4	***	0.561	0.576	0.579	0.583	0.587
153.4—143.4		0.593	0.611	0.614	0.619	0.624
143.4—133.4		0.630	0.650	0.654	0.659	0.665
133.4—123.4		0.671	0.694	0.699	0.705	0.712
123.4—113.4		0.718	0.745	0.751	0.758	0.766
113.4—103.4		0.772	0.804	0.811	0.819	0.828
103.4—93.4		0.833	0.873	0.881	0.891	0.902
93.4—83.4		***	0.953	0.964	0.976	0.990
83.4—73.4			1.049	1.063	1.078	1.096
73.4—63.4			1.165	1.182	1.202	1.226
63.4—58.4			1.267	1.289	1.315	1.355
58.4—53.4			***	1.370	1.400	1.435
53.4—48.4				***	1.496	1.538
48.4—43.4					***	1.654
						***

Table 2. continued

$d$	38. 4—33. 4	33. 4—31. 4	31. 4—29. 4	29. 4—27. 4	27. 4—25. 4	25. 4—23. 4
313. 4—303. 4	0. 314	0. 315	0. 316	0. 317	0. 318	0. 319
303. 4—293. 4	0. 324	0. 325	0. 326	0. 327	0. 328	0. 329
293. 4—283. 4	0. 335	0. 336	0. 337	0. 338	0. 339	0. 340
283. 4—273. 4	0. 347	0. 348	0. 349	0. 350	0. 351	0. 352
273. 4—263. 4	0. 359	0. 360	0. 361	0. 363	0. 364	0. 365
263. 4—253. 4	0. 372	0. 374	0. 375	0. 376	0. 378	0. 379
253. 4—243. 4	0. 387	0. 388	0. 390	0. 391	0. 392	0. 394
243. 4—233. 4	0. 402	0. 404	0. 405	0. 407	0. 408	0. 410
233. 4—223. 4	0. 419	0. 421	0. 422	0. 424	0. 429	0. 428
223. 4—213. 4	0. 437	0. 440	0. 441	0. 443	0. 445	0. 447
213. 4—203. 4	0. 457	0. 460	0. 461	0. 463	0. 465	0. 468
203. 4—193. 4	0. 479	0. 482	0. 484	0. 486	0. 488	0. 491
193. 4—183. 4	0. 503	0. 506	0. 508	0. 510	0. 513	0. 516
183. 4—173. 4	0. 530	0. 533	0. 535	0. 538	0. 541	0. 544
173. 4—163. 4	0. 559	0. 563	0. 566	0. 568	0. 572	0. 575
163. 4—153. 4	0. 592	0. 597	0. 599	0. 603	0. 606	0. 610
153. 4—143. 4	0. 630	0. 634	0. 638	0. 641	0. 645	0. 650
143. 4—133. 4	0. 672	0. 677	0. 681	0. 685	0. 690	0. 695
133. 4—123. 4	0. 720	0. 726	0. 730	0. 735	0. 741	0. 747
123. 4—113. 4	0. 775	0. 782	0. 788	0. 793	0. 800	0. 807
113. 4—103. 4	0. 839	0. 848	0. 854	0. 861	0. 869	0. 878
103. 4—93. 4	0. 915	0. 926	0. 934	0. 942	0. 951	0. 962
93. 4—83. 4	1. 006	1. 020	1. 029	1. 036	1. 051	1. 064
83. 4—73. 4	1. 117	1. 134	1. 145	1. 158	1. 173	1. 190
73. 4—63. 4	1. 253	1. 276	1. 291	1. 308	1. 327	1. 350
63. 4—58. 4	1. 379	1. 407	1. 426	1. 448	1. 484	1. 500
58. 4—53. 4	1. 477	1. 524	1. 533	1. 558	1. 600	1. 621
53. 4—48. 4	1. 588	1. 628	1. 656	1. 686	1. 721	1. 779
48. 4—43. 4	1. 715	1. 765	1. 799	1. 836	1. 879	1. 929
43. 4—38. 4	1. 861	1. 924	1. 967	2. 014	2. 068	2. 131
38. 4—33. 4	***	2. 110	2. 165	2. 226	2. 296	2. 377
33. 4—31. 4		***	2. 324	2. 400	2. 486	2. 585
31. 4—29. 4			***	2. 509	2. 607	2. 720
29. 4—27. 4				***	2. 739	2. 869
27. 4—25. 4					***	3. 033
25. 4—23. 4						***

Here,  $v_{12}$  is the total volume of nitrogen adsorbed in the pressure range of consideration;  $V_d d$ , the volume of pores having diameters between  $(d - \frac{1}{2}d)$  and  $(d + \frac{1}{2}d)$ ;  $d_{max}$ , the diameter of the largest pore. The values of  $k_{12}$  and  $R_{12}$  are given in the third and fourth columns of Table 1 for suitable pore-diameter

increments, and the factor  $(d-2t)/d^2$  is given in Table 2 for values of  $d$  larger than  $d_2$ . The second term in the bracket of equation (4) represents the volume of the nitrogen which increases the thickness of the adsorbed layer on the walls of larger vacant pores.

Since equation (4) can be applied to the de-

Table 3. Calculation of pore-size distribution of a silica gel (Davidson 59)

$d$ (Å)	$P/P_0$	$v_{12}$ (ml/g)	$v_{12} - k_{12} \Sigma$ (ml/g)	$V_{12}$ (ml/g)	$\Sigma V_{12}$ (ml/g)	$S_{12}$ (m <sup>2</sup> /g)	$\Sigma S_{12}$ (m <sup>2</sup> /g)
313.4	0.931	0.0010	0.0010	0.0012		0.156	
303.4	0.929	0.0013	0.0012	0.0015	0.0012	0.202	0.156
293.4	0.926	0.0015	0.0015	0.0018	0.0027	0.252	0.358
283.4	0.924	0.0018	0.0017	0.0021	0.0045	0.306	0.610
273.4	0.921	0.0018	0.0017	0.0021	0.0066	0.318	0.916
263.4	0.918	0.0015	0.0015	0.0018	0.0087	0.284	1.234
253.4	0.915	0.0035	0.0035	0.0043	0.0105	0.692	1.518
243.4	0.911	0.0033	0.0032	0.0040	0.0148	0.671	2.210
233.4	0.907	0.0050	0.0050	0.0062	0.0188	1.087	2.881
223.4	0.902	0.0061	0.0061	0.0077	0.0250	1.402	3.968
213.4	0.897	0.0100	0.0099	0.0126	0.0327	2.418	0.370
203.4	0.891	0.0116	0.0115	0.0147	0.0453	2.972	7.788
193.4	0.885	0.0153	0.0151	0.0196	0.0600	4.157	10.760
183.4	0.879	0.0281	0.0279	0.0364	0.0796	8.160	14.917
173.4	0.871	0.0631	0.0627	0.0828	0.1160	19.663	23.077
163.4	0.861	0.2246	0.2237	0.3028	0.1988	76.471	42.740
153.4	0.850	0.1967	0.1840	0.2664	0.5016	71.802	119.211
143.4	0.838	0.0835	0.0788	0.1098	0.7680	31.791	191.013
133.4	0.824	0.0515	0.0456	0.0648	0.8778	20.189	222.804
123.4	0.809	0.0263	0.0193	0.0279	0.9426	9.433	242.993
113.4	0.787	0.0288	0.0207	0.0307	0.9705	11.337	252.426
103.4	0.764	0.0288	0.0195	0.0296	1.0012	12.028	263.763
93.4	0.734	0.0225	0.0116	0.0182	1.0308	8.222	275.791
83.4	0.696	0.0250	0.0119	0.0192	1.0490	9.811	284.013
73.4	0.646				1.0682		293.824

sorption branch as well as to the adsorption branch, it is applied to the desorption branches of silica gel (Davidson 59), silica alumina (steam deactivated), and silica gel (Mallinckrodt Standard Luminescent). The procedure of pore volume distribution calculation adopted in this work is the same as the one proposed by Cranston and Inkley except the correction of the curvature dependency of surface tension. The adsorption isotherm for the above three samples have been reported previously by Cranston and Inkley<sup>2</sup>, and Brunauer et al<sup>8</sup>. The typical result of calculation for Davidson 59 is given in Table 3. The sixth column of the Table 3 is the cumulative volume. The seventh column is the inner surface area in square meters per gram of adsorbent, which can be obtained from the fifth column by the use of following equation;

$$S_{12} = \frac{4aV_{12}}{d'} \times 10^4$$

where,  $d'$  is the mean diameter of the corresponding region, and " $a$ " is a factor,  $1,584 \times 10^{-3}$ , which results from the geometrical consideration of close packing. The last column of the table is the cumulative surface area.

### The Result and Discussions

From Table 3, cumulative pore volume  $V(r)$  is plotted against pore radius  $r$ . The pore volume distribution curve, then, can be obtained by converting this plot to the  $\Delta V(r)/\Delta r$  versus  $r$  curve. Figures 1, 2, and 3 are the pore volume distribution curves obtained in this way for the three samples. In each figure, both results, one with curvature dependency correction and the other without correction, are shown for comparison. The result with curvature correction is quite similar in its shape to the one without correction, but the maximum

has shifted to the larger pore radius side.

The result of this shifting has significant meanings; firstly, the pore volume distribution calculated by the previous method gives a comparatively large negative deviation. In the case of silica alumina, the mean pore radius calculated by the proposed way is about 20 Å, while the previous method gives 15 Å. This is quite a large relative difference. Secondly, if the curvature dependency of surface tension is taken into account, the micro pore condensation occurs at the further lower relative vapor pressure than that accepted before. In other words, the vapor pressure in equilibrium with the condensate in the pore of given radius would be quite different from the vapor pres-

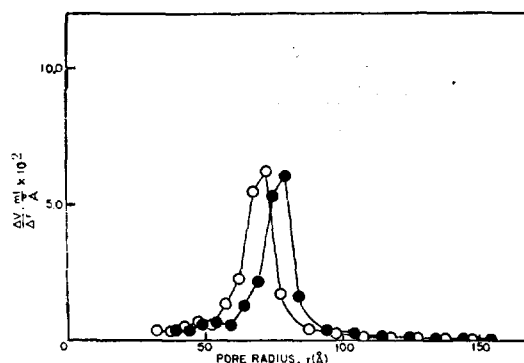


Fig. 1. Pore volume distribution of a silica gel (Davidson 59); ● corrected; ○ uncorrected.

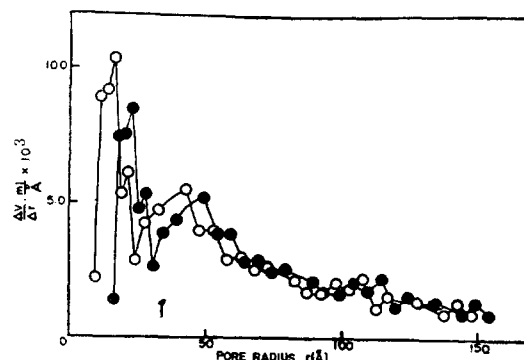


Fig. 2. Pore volume distribution of a silica gel (Mallinckrodt Standard Luminescent): ● corrected; ○ uncorrected.

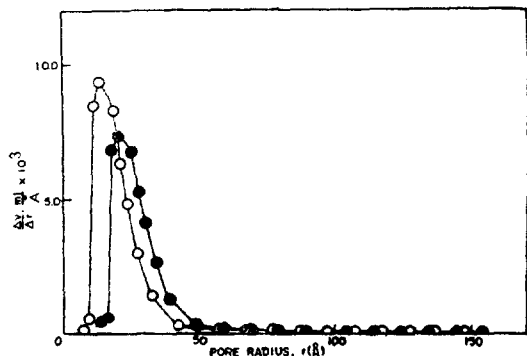


Fig. 3. Pore volume distribution of a silica alumina (heat deactivated); ● corrected; ○ uncorrected.

ure calculated assuming the surface tension is constant. This discrepancy becomes more prominent as the pore radius approaches to the lower limit of the transition pore. For example, when the pore diameter is about 30 Å, relative vapor pressure in equilibrium with the pore condensate is less than 0.13 as can be seen in Table 1, whereas it is 0.35 if the surface tension is assumed to be independent of the curvature.

As can be seen from Figures 2 and 3, silica gel (Mallinckrodt) and silica alumina have both transition and micro pores. This result coincide with the  $t$ -plot obtained by Brunauer et al<sup>8</sup>. Although the calculations are performed to the micro pore region, it is meaningless but for the purpose of comparison. It is inadequate to apply the thermodynamically derived Kelvin

equation to the micro pores. For Davidson 59, the cumulative surface area is 332.7 m<sup>2</sup>/g according to Cranston and 335 m<sup>2</sup>/g according to the corrected medelless method of Brunauer. The observed B.E.T. area is 273 m<sup>2</sup>/g. The cumulative surface area calculated by the proposed way is very close to the B.E.T. area, being 293.8 m<sup>2</sup>/g. The comparison of cumulative surface area of the other two samples to the B.E.T. area is meaningless as these adsorbents have micro pores.

The authors express their appreciation to the Ministry of Science and Technology for the grant of this work.

### References

1. E. P. Barrett, L. G. Joyner, and P. P. Halenda, *J. Amer. Chem. Soc.*, **73**, 373 (1951).
2. R. W. Cranston, and F. A. Inkley, *Advances in Catalysis*, **9**, 143 (1957).
3. S. Brunauer, R. Sh. Mikhail, and E. E. Bodor, *J. Colloid and Interface Sci.*, **24**, 451 (1967).
4. J. C. P. Broekhoff, and J. H. deBoer, *J. Catalysis*, **9**, 8 (1967).
5. R. C. Tolman, *J. Chem. Phys.*, **17**, 333 (1949).
6. J. G. Kirkwood, and F. P. Buff, *J. Chem. Phys.*, **17**, 338 (1949).
7. W. Ahn, M. Jhon, H. Pak, and S. Chang, *J. Colloid and Interface Sci.*, **38**, 605 (1972).
8. R. Sh. Mikhail, S. Brunauer, and E. E. Bodor, *J. Colloid and Interface Sci.*, **26**, 54 (1968).